www.czasopisma.pan.pl PAN POLSKA AKADEMIA NAUK www.journals.pan.pl

A R C H I V E S O F M E T A L L U R G Y A N D M A T E R I A L S

Volume 59 2014 Issue 1

DOI: 10.2478/amm-2014-0030

A. ROMANSKI*, J. KONSTANTY*

BALL-MILLED Fe-Ni AND Fe-Mn MATRIX POWDERS FOR SINTERED DIAMOND TOOLS

MIELONE PROSZKI Fe-Ni ORAZ Fe-Mn PRZEZNACZONE DO PRODUKCJI NARZĘDZIOWYCH MATERIAŁÓW METALICZNO DIAMENTOWYCH

The work presents the possibility of substitution of expensive, Co-WC powders, that have been traditionally used in the production of sintered diamond tools, with cheap iron-base counterparts manufactured by ball milling. It has been shown that ball-milled Fe-Ni and Fe-Mn powders can be consolidated to a virtually pore-free condition by hot pressing at 900°C. The as-consolidated materials are characterised by high hardness, bending strength and resistance to 3-body abrasion.

Keywords: ball milling, PM diamond tools, matrix, Fe-Ni, Fe-Mn, hot pressing

W pracy przedstawiono wyniki badań nad możliwością zastąpienia proszków Co-WC powszechnie stosowanych do produkcji spiekanych materiałów narzędziowych, tańszymi proszkami na bazie żelaza, otrzymanymi metodą mielenia w młynie kulowym. Stwierdzono, że spieki otrzymane z proszków Fe-Ni oraz Fe-Mn, które prasowano na gorąco w temperaturze 900°C, charakteryzują się małą porowatością, wysoką twardością i wytrzymałością na zginanie oraz dużą odpornością na zużycie ścierne w obecności 3 ciał.

1. Introduction

Over the past decades cobalt has been the most valued matrix metal in professional sintered diamond tools, such as saw blades, wire saws, core drills and grinding wheels used for cutting, drilling and shaping natural stone, concrete and ceramics. Like any other matrix material, cobalt combines excellent diamond retention and wear characteristics [1].

The strong position of cobalt had been unquestioned until the early 1990s when the collapse of the Zairean cobalt supply led to serious concerns about its price stability and initiated an extensive research on new powders [2]. The first cobalt substitutes were marketed under the brand names *Next* and *Cobalite* in 1997 and 1998 [3,4]. The new products complemented the variety of fine cobalt powders and continued to gain bigger market share which was increased to 25% in 2005 [5]. Although cobalt and its substitutes are still used for professional tools, the recent trend is towards a broader application of inexpensive, premixed [6,7,8] and mechanically alloyed iron-base powders [9].

2. Experimental procedure and results

Fe-Ni-Cu-Sn-C and Fe-Mn-Cu-Sn-C alloys manufactured from inexpensive ball-milled powders by the hot press route were chosen as potential cobalt substitutes in the manufacture of diamond impregnated segments for abrasive applications.

Spongy iron, prealloyed water atomised tin-bronze, milled ferromanganese, carbonyl nickel and synthetic graphite powders were provided by *Höganäs AB, ECKA, ESAB, Vale* and *Timcal*, respectively, and used as the starting powders (Fig. 1).

Prior to milling the powders were mixed in a *Turbula* type mixer for 10 minutes and ball-milled in air for 8 hours at 70% critical speed. About 50% of the milling container was filled with 12 mm hardened 100Cr6 steel balls and ~10:1 ball-to-powder weight ratio was used.

After ball milling the powders were examined metallographically. The powder compositions are provided in Tables 1 and 2, whereas the particle shapes and microstructures are shown in Fig 2.

TABLE 1

Chemical composition and particle size of starting powders

Powder grade	Chemical composition, wt.%						Particle size, μm
	Fe	Mn	Ni	Cu	Sn	C	
NC100.24	100	-	-	-	-	-	20-180
25GR80/20-325		-	-	80	20	-	11
FeMn affine	bal	80.8	-	-	-	1.3	0-500
FeMn high-carbon	bal	80	-	-	-	6.8	0-500
T210	-	-	bal	-	-	0.33	0.6
F10	-	-	-	-	-	100	0-10

* AGH UNIVERSITY OF SCIENCE AND TECHNOLOGY, AL. A. MICKIEWICZA 30, 30-059 KRAKÓW, POLAND

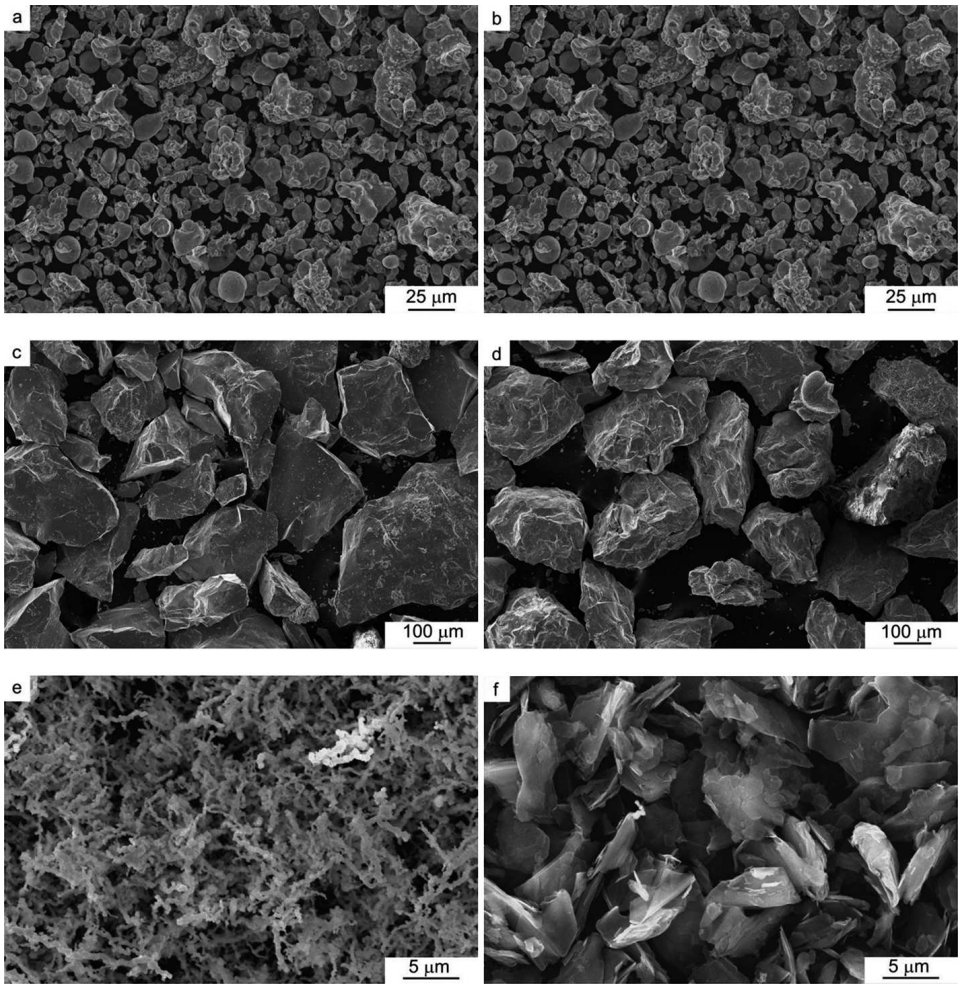

Fig. 1. Experimental powders: (a) NC100.24 iron, (b) 25GR80/20-325 bronze, (c) FeMn affine, (d) FeMn high-carbon, (e) T210 nickel and (f) TIMREX F10 graphite

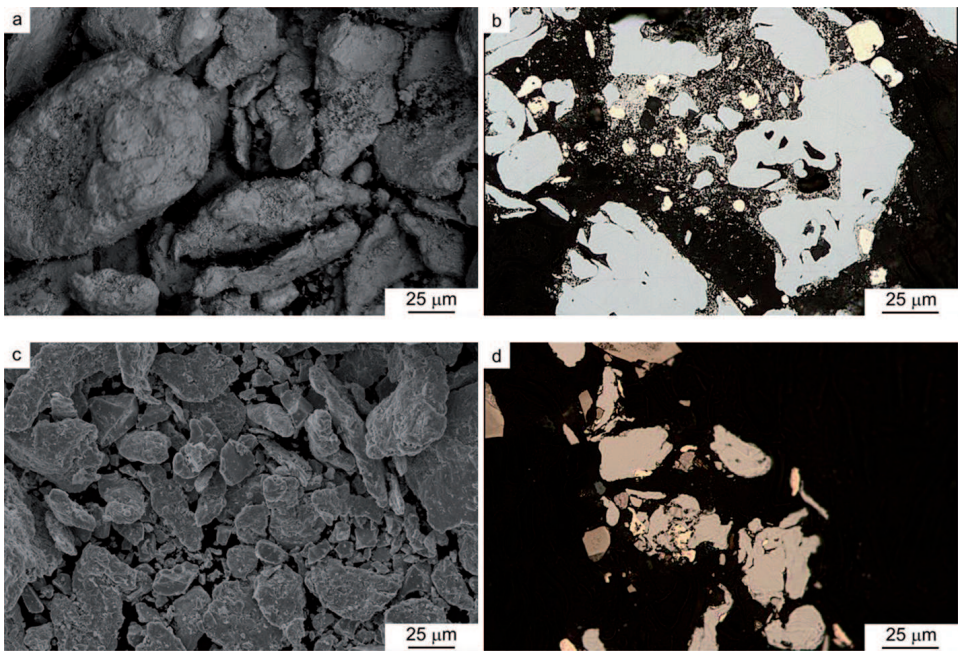

Fig. 2. Particle shape (a), (c) and microstructure (b), (d) of Fe-Ni and Fe-Mn powder, respectively

TABLE 2
Powder composition and chemical composition of ball-milled powders

Powder designation	Powder composition	Chemical composition, wt.%					
		Fe	Mn	Ni	Cu	Sn	C
Fe-Ni	T210 - 12% 25GR80/20-325 - 8% F10 - 0.63% NC100.24 - bal	bal	-	12	6.4	1.6	0.67
Fe-Mn	25GR80/20-325 - 8% FeMn affine - 7.5% FeMn high-carbon - 7.5% NC100.24 - bal	bal	12.1	-	6.4	1.6	0.6

Each ball-milled powder was then poured into four rectangular cavities of a graphite mould and consolidated to near-full density by passing an electric current through the mould under uniaxial compressive load. The powder was held for 3 minutes at 900°C, under 25 MPa (Fe-Ni) or 30 MPa (Fe-Mn), and subsequently cooled down at a mean rate of 6.4 K/s within the critical temperature range from the hot pressing temperature down to 550°C.

The as-consolidated bending specimens were first tested for density and hardness using the water displacement method and Knoop test, respectively. After subsequent 3-point bending test the broken test pieces were used to produce specimens for microstructural observations, chemical analysis (for oxygen and carbon) as well as for testing resistance to abrasive wear. The wear measurements were performed by means of the Micro Wear Test (MWT) [10,11], whereby an abrasive index (*Ai*), representing the average loss of height of the test piece per 20 m sliding distance, was calculated for abrasion by standardized quartz sand. In addition to the investigated Fe-Ni and Fe-Mn specimens, a commercial Co-20%WC PM alloy was tested as a reference material.

TABLE 3
As-consolidated densities, Knoop hardness numbers and bending properties of the experimental alloys (1)

Material	Density (g/cm^3)	KH1		3-point bending test		
		polished surface	abraded surface	TRS (MPa)	0.2% OYS (MPa)	ε_{pl} (%)
Fe-Ni	7.91-7.96	271±33	370±34	1161± 277	775± 178	2.01± 0.97
Fe-Mn	7.71-7.72	287±18	378±44	1086± 231	898± 98	0.88± 0.56

(1) scatter intervals estimated at 90% confidence level

It has been documented on annealed polycrystalline 70:30 brass [12] that both grinding and polishing produce a plastically deformed layer. Its depth depends on the sharpness and size of the abrasive, hence the deformed layer extends to 77 and 0.7 μm after plain grinding on #220 SiC paper and after fine polishing on 1 μm diamond respectively. More importantly, a significant plastic deformation occurs only after grinding and extends down to ~8 μm beneath a 2 μm thick, scratched skin. Therefore by using XRD with the Cu Kα_1 radiation in Bragg-Brentano geometry it was possible to determine the proportion of (γFe) to (αFe) in the subsurface layer of the diamond-polished metallographic specimens. Similar analysis was also carried out on the abraded surface of the wear test specimens in order to predict the amount of martensite which could be generated beneath the working face of the tool by abrasion.

The results of measurements are given in Tables 3 and 4 whereas the XRD patterns and microstructures are presented in Figs 3-6.

TABLE 4
Chemical analysis, resistance to abrasion and phase compositions of the experimental alloys

Material	Content of		Abrasive Index *Ai* (1) (μm/20m)	Percentage of austenite ($V_{(\gamma Fe)}$)(2)	
	oxygen (wt.%)	carbon (wt.%)		As-polished condition	As-ground condition
Fe-Ni	0.48	0.60	22.0±3.1	82.6	11.7
Fe-Mn	0.66	0.64	22.1±3.9	64.2	59.4
Co-20%WC	-	-	33.6±8.2	-	-

(1) scatter intervals estimated at 90% confidence level
(2) estimated assuming that $V_{(\alpha Fe)} + V_{(\gamma Fe)} = 100\%$ (no account taken of other phases)

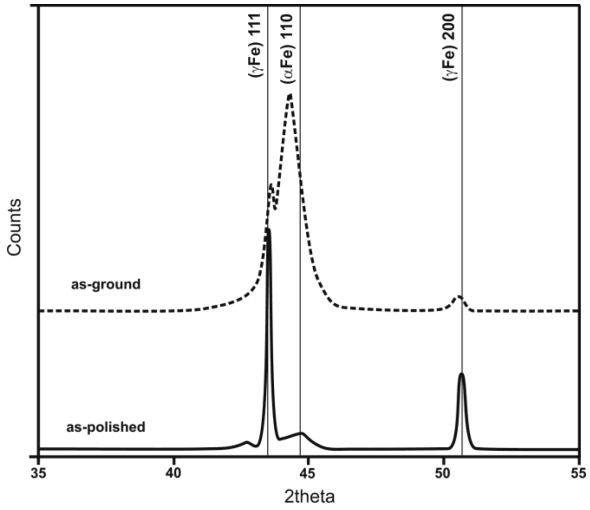

Fig. 3. XRD patterns of Fe-Ni alloy in as-polished and as-ground condition

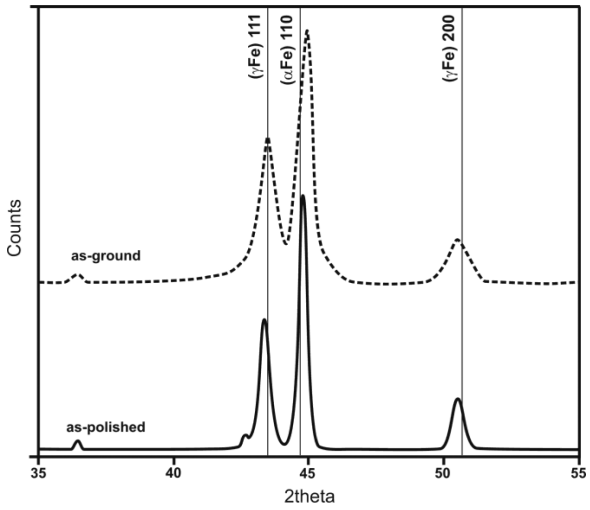

Fig. 4. XRD patterns of Fe-Mn alloy in as-polished and as-ground condition

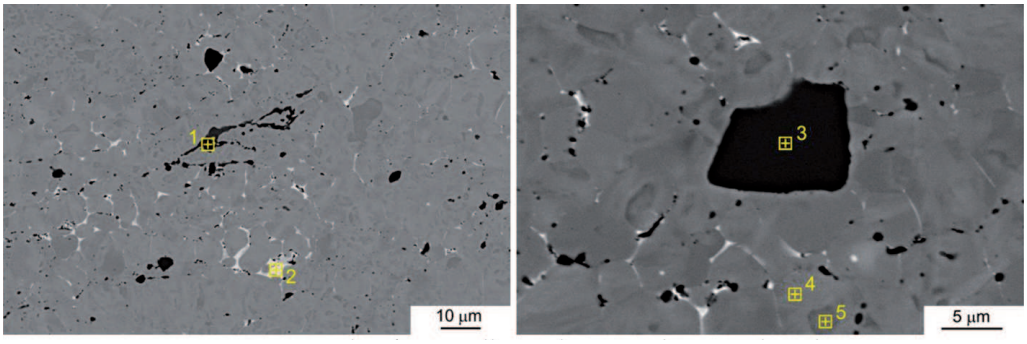

Fig. 5. SEM micrographs of Fe-Ni alloy and EDS analysis at selected areas (wt.%): 1 and 3: Fe_2O_3; 2: 52Cu-35Sn-8Ni-5Fe; 4: 82Fe-14Ni-4Cu; 5: Fe

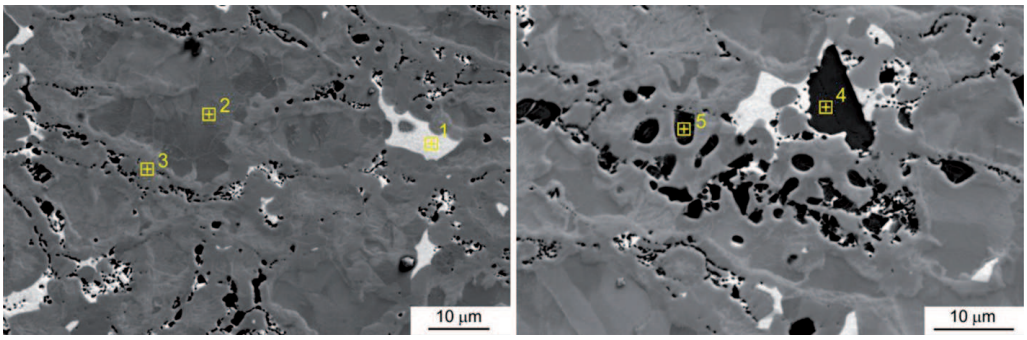

Fig. 6. SEM micrographs of Fe-Mn alloy and EDS analysis at selected areas (wt.%): 1: 64Cu-20Sn-12Mn-5Fe; 2: Fe; 3: 79Fe-19Mn-2Cu; 4 and 5: Mn_2O_3

3. Discussion and conclusions

The results given in Table 2 indicate that the powders ball-milled for 8 hours can be hot pressed to a virtually pore-free (closed porosity) condition by a 3-minute hold at 900°C under a pressure of 25-30 MPa. The addition of 8% Cu-20%Sn bronze to the powders prior to milling provides sufficient amount of liquid at 900°C to aid densification.

After densification the tested alloys possess high hardness and mechanical strength, comparable to other matrix materials [6,7,8,9]. The hardness markedly increases after deformation brought about by abrasion. From the XRD data included in Table 3 and in Figs 3, 4 it is evident that the Fe-Ni alloy strain hardens due to the abrasion-induced martensitic transformation (γFe)→ (αFe), whereas in the Fe-Mn alloy the retained austenite is stable. This suggests that other mechanisms, e.g. mechanical twinning [13], may contribute to its strain hardening.

During milling the Fe-Mn powder picks up more oxygen compared to its Fe-Ni counterpart which apparently results in lower ductility of the bending specimens (Table 3), however, it is noteworthy that none of them failed in a brittle manner.

As seen in Figures 5 and 6 both alloys display non-uniform, fine-grained microstructure. The EDS examinations of the metallographic sections revealed marked differences in microstructural inhomogeneity between the two alloys. Fe-Mn shows more inhomogeneous distribution of structural components with relatively coarse (αFe) areas (dark-gray phase in Figure 6) surrounded by a network of Fe-Mn alloy (bright-gray phase in Figure 6). In Fe-Ni the (αFe) areas are smaller and scarce (e.g. area 5 in Figure 5). It seems reasonable to assume that the alloying of iron with nickel and manganese starts with dissolving these elements in the melting bronze and spreading them with the liquid across the hot pressed specimens. Then they diffuse into the iron particles and, acting in concert with carbon, conserve the major part of austenite upon cooling to room temperature.

Interestingly, the tested iron-base alloys exhibit higher resistance to 3-body abrasion compared to the Co-20%WC reference material, which has found industrial application as a matrix in saw blade segments used to cut sandstone and abrasive ceramics. As with hardness the increased resistance of Fe-Ni to abrasive wear can be attributed to the formation of strain-induced, carbon-rich martensite. The Fe-Mn alloy has virtually the same wear resistance as Fe-Ni although only a negligible portion of austenite is transformable to martensite under tribological straining. Therefore a thorough insight into the Fe-Mn microstructure is still needed to explain the strain hardening mechanisms.

The main results of this study can be summarised as follows.

1. The investigated ball-milled powders can be readily consolidated to the closed porosity condition by a 3-minute hold at 900°C and under a moderate pressure of 25-30 MPa.
2. The as-sintered Fe-Ni and Fe-Mn materials combine high hardness (271-287 HK1) and transverse rupture strength (1086-1161 MPa) with acceptable ductility.
3. 8 wt.% addition of tin bronze to the powders prior to ball milling provides a liquid phase (>798°C) which aids consolidation and intensifies diffusion of nickel and manganese to iron, thereby increasing the amount of retained austenite.

4. The as-sintered Fe-Ni specimens contain almost 83% of retained austenite which readily transforms to martensite under tribological straining, thus increasing the alloy's hardness and resistance to abrasion.
5. The as-sintered Fe-Mn specimens contain around 64% of retained austenite which hardly transforms to martensite under tribological straining.
6. The Fe-Ni and Fe-Mn are characterised by markedly higher resistance to abrasion than the reference Co-20%WC alloy.

It should be noted that further studies are underway in order to explain the strain hardening mechanism and excellent wear characteristics of the Fe-Mn alloy.

Acknowledgements

The authors gratefully acknowledge Professor W. Ratuszek for her able assistance with the XRD measurements. The work was supported by the Polish Ministry of Science & Higher Education through contract 11.11.110.158.

Received: 20 April 2013.

REFERENCES

[1] J. Konstanty, Industrial Diamond Review **60**, 55 (2000).
[2] J. Konstanty, Powder Metallurgy **56**, 3 (2013).
[3] Anon., Marmomacchine International **18**, 156 (1997).
[4] I.E. Clark, B.-J. Kamphuis, Industrial Diamond Review **62**, 177 (2002).
[5] Anon., Industrial Diamond Review **65**, 45 (2005).
[6] J. Konstanty, T.F. Stephenson, D. Tyrala, Diamond Tooling Journal **3**, 26 (2011).
[7] D. Tyrała, Kształtowanie struktury i własności spieków Fe-Ni-Cu-Sn stanowiących osnowę w narzędziach metaliczno-diamentowych. PhD Thesis. AGH-University of Science & Technology, Krakow, 2010, April.
[8] J. Konstanty, D. Tyrała, A. Radziszewska, Archives of Metallurgy and Materials **54**, 1051 (2009).
[9] J. Konstanty, A. Romanski, Materials Sciences and Applications **3**, 779 (2012).
[10] K. Muller, E. Fundal, Wear Resistant Materials **2**, 481, Reutte (1989).
[11] E. Fundal, Structure **3**, 3 (1989).
[12] K. Geels, Structure **35**, 5 (2000).
[13] S. Allain, J.-P. Chateau, O. Bouaziz, S. Migot, N. Guelton, Materials Science and Engineering A **387-389**, 158 (2004).